

Alkali Metal Ion Selectivity of the Hemocyanin Channel

Ximena Cecchi, Ramon Latorre* and Osvaldo Alvarez

Departamento de Biología, Facultad de Ciencias Básicas y Farmacéuticas, Universidad de Chile, Santiago, Chile, and

*Department of Physiology and Biophysics, Harvard Medical School, Boston, Massachusetts 02115

Summary. The selectivity of the hemocyanin channel was measured for alkali metal ions and ammonium. Permeability ratios relative to K^+ measured from biionic potentials were: NH_4^+ (1.52) > Rb^+ (1.05) > K^+ (1.0) > Cs^+ (0.89) > Na^+ (0.81) > Li^+ (0.35). Single-channel ion conductance was a saturating function of ion concentration regardless of the cation present in the bathing medium. Maximal conductances were 270, 267, 215, 176, 170 and 37 pS for K^+ , Rb^+ , NH_4^+ , Cs^+ , Na^+ and Li^+ , respectively. Current-voltage curves for the different monovalent cations were measured and described using a three-barrier model previously used to explain the voltage dependence of the “instantaneous” channel conductance (Cecchi, Alvarez & Latorre, 1981). In this way, binding and peak energies were estimated for the different ions. Considering the energy peaks as transition states between the ion and the channel, it is concluded that they follow Eisenman’s selectivity sequences XI (cis peak, i.e., $Li^+ > Na^+ > K^+ > Rb^+ > Cs^+$; highest field strength), VII (central peak) and II (trans peak). The cis side was that to which hemocyanin was added and was electrically ground. The binding energies, on the other hand, follow Eisenman’s series XI for strong electric field sites. Binding of NH_4^+ to the cis-well suggests that the orientation of the ligands in the site is tetrahedral.

Key Words hemocyanin · channel selectivity · energy barriers · ion transport

Introduction

Keyhole limpet hemocyanin interacts with lipid bilayer membranes increasing their conductance by several orders of magnitude (Pant & Conran, 1972). We have shown that ion conductance is mediated by ionic channels formed by hemocyanin in the membrane (Alvarez, Diaz & Latorre, 1975). The channels are cation selective and ideally exclude divalent anions like sulfate. Single-channel conductance measurements using various cations reveal that molecules the size of tetramethylammonium (TMA), with a diameter of 0.6 nm cannot pass through the channel (Cecchi et al., 1982). This result is consistent with the reflection coefficients of nonelectrolytes in bilayers containing hemocyanin which demonstrate that molecules the size

of acetamide ($0.4 \times 0.6 \times 0.6$ nm) are excluded from the channel. Furthermore, electrokinetic experiments designed to determine the interaction of water and ions in the channel indicate that three water molecules are associated with each ion that moves through the hemocyanin channel (Cecchi et al., 1982). From these characteristics, we concluded that the hemocyanin channel has a region that behaves as a filter which can be described as a cylinder 0.6 nm in length and 0.5 nm in diameter. All these results suggest that hemocyanin forms narrow pores where the ion conduction mechanism is more complicated than ion diffusion in water. For example, conductance is a saturating function of ion concentration; there is competition for the channel ion-binding sites when different permeant ions are present at the same time; and conductance is a nonlinear function of membrane potential. We have reported a three-barrier model based on the Eyring absolute rate theory which successfully accounts for these properties of the hemocyanin channel (Cecchi et al., 1981). The same model is used here to explain alkali metal ion selectivity and permeability sequences measured for this channel. In the three-barrier model, only one ion is allowed to occupy the channel at any given time. Two binding sites are represented by two energy wells which are separated from each other and from the surrounding solutions by three energy barriers. The energy change for a given ion going from the aqueous solution to the interior of the channel can be estimated from the hemocyanin-induced current-voltage curves. We found that the binding series is $Li^+ > Na^+ > K^+ > Rb^+ > Cs^+$ which corresponds to Eisenman’s series XI (Eisenman, 1965). We conclude that the two binding sites of the hemocyanin channel behave as strong electric field binding sites for cations. By extending the theory of selectivity to the energy

peaks (e.g., Hille, 1975; Eisenman & Horn, 1983), we found that from cis to trans side they follow Eisenman's sequences XI, VII ($\text{Na}^+ > \text{K}^+ > \text{Rb}^+ > \text{Cs}^+ > \text{Li}^+$) and II ($\text{Rb}^+ > \text{Cs}^+ > \text{K}^+ > \text{Na}^+ > \text{Li}^+$), respectively.

Materials and Methods

Membranes were formed by apposition of two monolayers in the presence of decane which is necessary for the hemocyanin interaction with the bilayer (Alvarez et al., 1975). Monolayers were spread from hexane/decane = 0.95/0.05 solutions of soybean lipids and cholesterol. The composition of the membrane solution was 10 mg/ml soybean lipids, and 5 mg/ml cholesterol. All components of the membrane solution were obtained from Sigma Chemical Co. (St. Louis, Mo.). Current was measured with a two-electrode voltage clamp as described previously (Alvarez & Latorre, 1978).

Single-channel conductance was measured using sulfate salts of the different cations to avoid contribution of anionic currents. Once the membrane was formed, hemocyanin from the keyhole limpet *Megatura crenulata* (Calbiochem-Behring Corp., San Diego, Calif.) was added to only one side of the membrane, the cis side, which was also electrically ground. Membrane potential was held at -50 mV and current was continuously recorded. Current increased in discrete steps each time a hemocyanin channel was incorporated into the membrane. Single-channel conductance was measured from the amplitude of at least 20 of these current jumps.

Current-voltage curves were measured when a large number of channels was incorporated in the membrane. We used a train of short square voltage pulses of increasing amplitude to measure the current-voltage relationship to avoid hysteresis due to the slow current relaxation of the channels at large positive potentials (Alvarez et al., 1975). Current samples were taken one millisecond after the onset of each pulse. Current-voltage curves consisted of 250 points taken at 2 mV intervals, spanning a voltage range from -250 to +250 mV. Several sweeps (>20) from at least three different membranes were accumulated and the resulting current values were scaled down to the current of a single channel using the single-channel conductance obtained at -50 mV.

Permeability ratios were calculated from the zero current potential developed when the membrane separated two solutions containing different cation solutions of the same concentration. The permeability ratio (P_y/P_x) was defined in terms of the zero current potential (V_0) as:

$$P_y/P_x = \exp(-FV_0/RT)$$

where F , R and T have their usual meanings. For these experiments, membranes were formed under asymmetric solutions, the cis side containing 50 mM K_2SO_4 , and the trans side containing 50 mM Rb^+ , NH_4^+ , Cs^+ , Na^+ or Li^+ sulfate. Both solutions were buffered with 5 mM Tris Cl (pH 7). Hemocyanin was added to the cis side only and membrane conductance was continuously monitored. When it reached at least 0.1 μS , the open-circuit transmembrane potential was measured by means of a high input impedance electrometer (model 602, Keithley Instruments, Cleveland, Ohio). The membrane was then broken by tapping the chamber and the potential in the absence of the membrane was recorded. The measured potential was corrected for the liquid junction potential which was calculated by using the Henderson equation (Lakshminarayanaiah, 1969).

The parameters for the three-barrier model were calculated by an iterative computer program which searched for the best nonlinear fit of the curves using the least-square criterion. Standard deviation of each parameter was calculated from the incidence of changes of the parameter on the sum of squares. The model has been fully described elsewhere (Cecchi et al., 1981) and is shown in the inset of Fig. 2. Briefly, ion transport was modeled as a series of jumps over three energy barriers and two binding sites in the channel. Only one ion was allowed to reside in the channel at any given time. Rate constants for ion movement were functions of the energy values at the peaks and wells which were in turn functions of the local electric potential. The positions in the electric field of the central energy barrier and one of the wells were adjustable, giving a total of seven free parameters in the curve-fitting procedure. Once the position parameters were obtained from preliminary runs of the program, these values became fixed parameters common to all ions used. The values of the different parameters are reported as the most likely values with their standard deviation.

Results

SINGLE-CHANNEL CONDUCTANCE

Single-channel conductances obtained at -50 mV for different ions are plotted in Fig. 1 as a function of cation activity. The saturating functions can be approximated by rectangular hyperbolas from which the maximum conductance (G_m) and the concentration for half-maximum conductance (K_m) can be calculated. These parameters are listed in Table 1. The selectivity sequence for G_m is $\text{K}^+ \simeq$

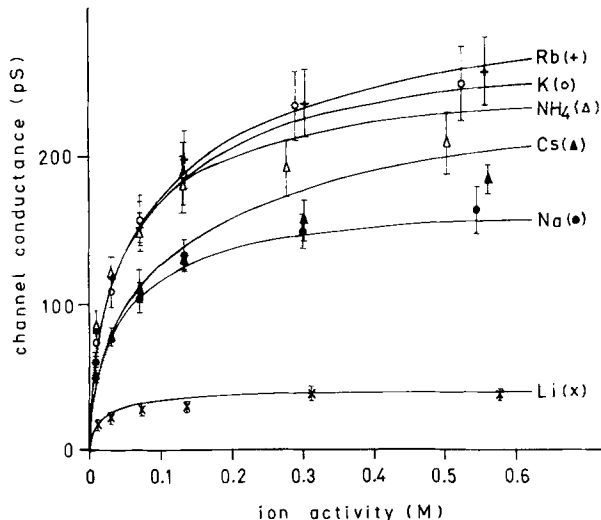


Fig. 1. Single-Channel Conductance. Membrane was formed under the appropriate sulfate salt of indicated cations. Hemocyanin was added to one side of the membrane and the potential of the other side was held at -50 mV. Current was continuously recorded and the sudden jumps associated with channel formation were measured. Bars represent one standard error of the averages. The solid lines are the expected conductance-concentration curves calculated from the three-barrier model using the parameters in Table 2

Table 1. Single-channel conductance and permeability ratios

Ion (X)	G_m (pS)	K_m (mM)	P_X/P_K		$(K_m X/K_m K)(P_X/P_K)$ ($G_m X/G_m K$)
			exp	model	
Li^+	37 (4)	25.6(9.8)	0.35(0.01)	0.51(0.08)	1.30(0.51)
Na^+	170 (7)	37.5(5.6)	0.81(0.01)	0.82(0.13)	0.99(0.17)
K^+	270 (6)	48.8(3.5)	1.00	1.00	1.00
Rb^+	267(12)	43.3(6.5)	1.05(0.03)	1.16(0.13)	0.94(0.16)
Cs^+	176 (8)	37.4(5.9)	0.89(0.03)	0.77(0.12)	1.05(0.17)
NH_4^+	215 (6)	26.4(2.0)	1.52(0.03)	1.30(0.16)	1.03(0.14)

Maximum channel conductance G_m and the apparent dissociation constant K_m for the different cations were obtained by fitting a hyperbolic function to the conductance concentration points. The values shown are the mean parameters and their standard deviation is shown in parentheses. Permeability ratios (exp) were obtained from the zero current potential under biionic conditions, always having K^+ at the hemocyanin side of the membrane, as explained in Materials and Methods. They are compared with the ratios calculated from the three-barrier model. Values are the mean of at least three determinations.

$\text{Rb}^+ > \text{NH}_4^+ > \text{Cs}^+ \text{Na}^+ > \text{Li}^+$. For K_m the sequence is $\text{K}^+ > \text{Rb}^+ > \text{Na}^+ \sim \text{Cs}^+ > \text{NH}_4^+ > \text{Li}^+$.

ZERO CURRENT POTENTIALS

The permeability ratios are measured from the zero current potentials developed on hemocyanin-treated membranes separating solutions of different ion composition. However, hemocyanin channels present several conductance states which appear with different probabilities as a function of membrane potential (Latorre et al., 1975; Menestrina, Maniacco & Antolini, 1983). Therefore, if during the experiment a change from one conductance state to another occurs, interpretation of the results becomes difficult. The potentials developed during these experiments ranged between +1 and -25 mV, on the hemocyanin-containing side. At these potentials, the hemocyanin channel is open all the time; all the conclusions, therefore, refer to the fully open channel. We have chosen potassium as the reference ion to evaluate the permeability ratios and these, relative to K^+ , are listed in Table 1. $\text{NH}_4^+ > \text{Rb}^+ > \text{K}^+ > \text{Cs}^+ > \text{Na}^+ > \text{Li}^+$ is the selectivity sequence given by this method for alkali metal ions.

CHANNEL CONDUCTANCE AND PERMEABILITY

We now have two different selectivity sequences as the result of two different experimental approaches. In particular, in a channel that can be occupied by at most one ion at a time this is to be expected inasmuch as K_m is solely a function of the well free energies, whereas G_m is a function of both peak and well free energies (Lauger, 1973; Coronado, Rosenberg & Miller, 1980). The biionic potentials, on the other hand, depend only on peak heights. Furthermore, models restricted to single

ion occupancy and constant peak energy offset predict a definite relationship for G_m , K_m and permeability. Specifically, the product of the permeability ratios and the K_m ratios divided by the G_m ratios must be equal to one for all ions (Hille, 1975; Coronado, Rosenberg & Miller 1980). This relation is followed approximately by the hemocyanin channel as can be seen in Table 1, which does not however imply that both conditions are being fulfilled (see Discussion below).

CURRENT-VOLTAGE CURVES

Different selectivity sequences are found when single-channel conductances are measured at different potentials. Figure 2 shows the current as a function of potentials for the different ions at 100 meq/liter. The sequence is $\text{NH}_4^+ > \text{Rb}^+ > \text{K}^+ > \text{Cs}^+ > \text{Na}^+ > \text{Li}^+$ for large negative potentials and changes to $\text{NH}_4^+ > \text{Rb}^+ > \text{Cs}^+ > \text{K}^+ > \text{Na}^+ > \text{Li}^+$ for large positive potentials. To describe the current-voltage curves we have modeled the transport of the ion through the channel as a series of jumps over energy barriers separating energy wells, as diagrammatically presented in the inset of Fig. 2. The three-barrier model assumes that there is a barrier near the center of the channel separating two wells. The additional barriers separate the wells from the surrounding aqueous solutions. When an electric potential V is established across the membrane, the potential at the cis side barrier does not change. On the other hand, the cis side well "feels" a fraction of the applied potential equal to $D_1 V$, where D_1 is the fractional electrical distance (see inset of Fig. 2). The central barrier feels a fraction of the applied potential equal to $D_2 V$ and the full applied potential is present at the trans side well and barrier. The height of the central barrier is

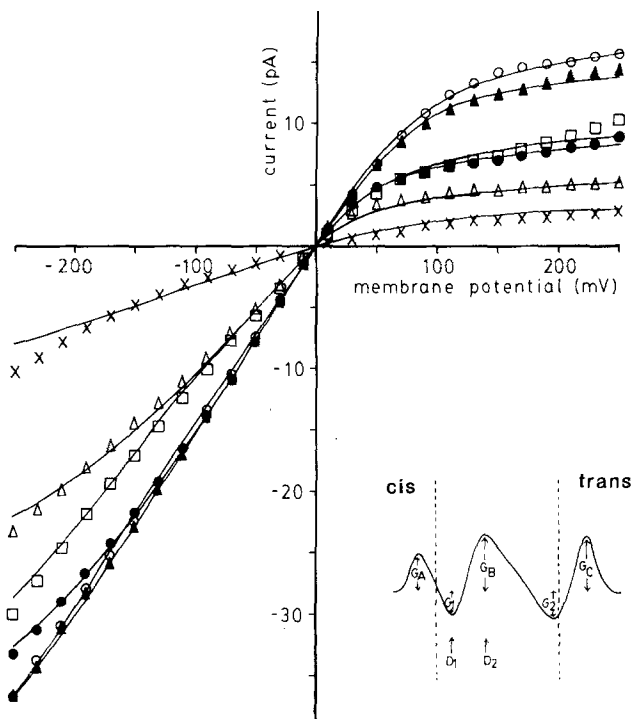


Fig. 2. Current-Voltage Curves. These curves are obtained in membranes with many hemocyanin channels using 100 meq/liter sulfate solutions of the different cations. Current was measured one millisecond after the onset of a voltage pulse of the indicated amplitude. Each point in the graph is the result of the addition of at least 20 determinations in three different membranes. The original curves have a resolution of 2 mV. Data were reduced to 20 mV resolution taking the average values around each potential. Currents are scaled down to the single-channel conductance to allow for comparison of different ions and to use in the model curve fitting. The lines in the graph are the expected currents from the three-barrier model calculated using the parameters in Table 2. K^+ (●); Rb^+ (▲); Cs^+ (□); NH_4^+ (○); Na^+ (△); Li^+ (×). Inset: diagrammatic representation of the three-barrier model. G_1 and G_2 , reduced free energies of ions at binding sites 1 and 2. G_A , G_B and G_C reduced energies of the ions at the energy barriers. D_1 and D_2 , electric constants of central barrier and well 1, respectively. They were set at $D_1 = 0.152$ and $D_2 = 0.338$ (see text) from the cis side. G_A and G_C are set away from the membrane because we found previously (Cecchi et al., 1981) that these barriers are independent of the surface potential.

G_B and those of the external barriers are G_A and G_C . The depth of the wells are represented by G_1 and G_2 . To find these seven parameters, we used a least-squares nonlinear curve-fitting procedure. The result of the curve-fitting process is in Table 2. The lines in Fig. 2 were calculated using the energy values listed in Table 2. Further, we have shown that at least for K^+ and Li^+ this model is useful to describe the $I-V$ curves for several concentrations (Cecchi et al., 1981).

From the data in Table 2, we conclude that the sequence of binding energies of ions to the wells is $Li^+ > Na^+ > K^+ > Rb^+ > Cs^+$. For the peaks, we obtained the following selectivity sequences: G_A : $Li^+ > Na^+ \sim K^+ > Rb^+ > NH_4^+ > Cs^+$; G_B : $Na^+ > K^+ > NH_4^+ > Rb^+ > Cs^+ > Li^+$; G_C : $NH_4^+ > Rb^+ > Cs^+ \sim K^+ > Na^+ > Li^+$. Furthermore, the peak energies depart from the constant offset condition.

The significance of this curve-fitting procedure and the usefulness of the model can be tested by the prediction of the conductance values in the concentration plane. The solid curves in Fig. 1 show the conductance as a function of ion concentration as calculated from the parameters in Table 2. To calculate these conductances, it is necessary to introduce the variation that the parameters suffer as the membrane surface potential changes with ionic strength inasmuch as the soybean lipid membranes bear a negative surface charge. We used the surface potential variations and the parameter dependence on surface potential reported in the original statement of the model (Cecchi et al., 1981). Figure 1 shows that the model is in reasonable agreement with the experimental data. Table 1 shows a comparison between the permeability ratios measured and those calculated from the model. The calculated values are close to the experimental, which is another independent test of the applicability of this model as a description of ion transport through the hemocyanin channel.

Table 2. Energy parameters for the three-barrier model

Ion	G_1	G_2	G_A	G_B	G_C
Li^+	-2.01(0.04)	-0.94(0.08)	2.89(0.12)	5.65(0.03)	5.76(0.06)
Na^+	-1.69(0.04)	-0.50(0.03)	3.77(0.05)	5.05(0.04)	5.56(0.02)
K^+	-1.26(0.02)	-0.41(0.01)	3.63(0.02)	5.11(0.01)	5.38(0.09)
Rb^+	-1.04(0.03)	-0.32(0.02)	3.88(0.02)	5.32(0.01)	5.09(0.01)
Cs^+	-0.99(0.07)	1.09(0.09)	4.39(0.05)	5.61(0.05)	5.38(0.02)
NH_4^+	-1.31(0.02)	-0.22(0.01)	3.91(0.02)	5.24(0.02)	4.96(0.05)

Current-voltage curves were measured in membranes treated with hemocyanin using 100 meq/liter sulfate solutions of the indicated cation. At least 24 curves were added for each cation. The voltage interval used was ± 250 mV. Current was normalized for the single ion current at -50 mV measured for each ion in separate experiments. The parameters in the Table were obtained from a least squares curve-fitting computer program, position parameters were forced to be the same for all ions: 0.152 for D_1 and 0.338 for D_2 . See Fig. 2 for description of the parameters. Energy values in this Table are in kcal/mole. Numbers in parentheses are the standard deviation of the parameter.

Discussion

GENERAL

Ion transport through the hemocyanin channel is a complicated function of ion concentration, electric potential and time. The time dependence of the conductance arises from molecular changes of the channel which take place in a time scale on the order of seconds. In what follows, we consider only time independent (instantaneous) processes. The voltage dependence of the open-channel conductance is well described by a three-barrier model based on absolute reaction rate theory. The model can also account for the conductance as a function of ion concentration for all ions studied, and for the biionic potentials arising when the membrane separates solutions containing different sulfate salts.

A different view of ion conduction and selectivity through the keyhole limpet hemocyanin channel has been proposed by Antolini and Menestrina (1979). They view the channel as a large pore (~ 30 nm in diameter) in which cations move as in free solution. At least four independent experimental results presented in this work and elsewhere (Cecchi et al., 1981; 1982) strongly suggest that this is not the case: (a) The selectivity sequences for the alkali cations obtained from conductance and zero current potential measurements are *not* those expected for a large aqueous pore. In both cases, Cs^+ is out of place; i.e., $\text{Rb}^+ > \text{K}^+ > \text{Cs}^+$ from biionic potentials and $\text{K}^+ > \text{Rb}^+ > \text{Cs}^+$ from conductance measurements. We note here that Antolini and Menestrina did not measure the Cs^+ conductance through the channel. Further, the Li^+ permeability is lower (\sim twofold) than that expected from the free diffusion in water (Alvarez, Reyes & Latorre, 1977; Antolini & Menestrina, 1979). (b) We found no measurable permeability for TMA through the channel. TMA has a diameter of about 0.6 nm (Cecchi et al. 1982). (c) The nonelectrolyte acetamide ($d \sim 0.5$ nm) is excluded from the hemocyanin channel (Cecchi et al., 1982). (d) We found it difficult to reconcile the fact that the instantaneous current-voltage relationships show a high degree of rectification (see Fig. 2 and Cecchi et al., 1981) with ions moving in free solution in the channel. We expect no rectification in the latter case.

THE HEMOCYANIN CHANNEL DOES NOT FOLLOW THE CONSTANT PEAK ENERGY OFFSET

The basis of the model is the assumption that only one ion can occupy the channel at a time. In the

present work, we tried to test this assumption using the relation $(K_m X / K_m K)(P X / P K) / (G_m X / G_m K)$, which should be unity for all ions in channels with single-ion occupancy and constant peak energy offset (Hille, 1975; Coronado et al., 1980). It is remarkable that this relation is unity for the hemocyanin channel even though the energy values for the maxima do not change in the same magnitude from one ion to another. However, we believe that finding a value of unity for the above-mentioned relation is of limited significance in the case of the hemocyanin channel. This is so because its selectivity is not dramatic or, in other words, conductances and permeabilities for the different monovalent cations tested here are of the same order of magnitude. To illustrate this point, we have calculated the expected $K_m - P - G_m$ relationship using the three-barrier model and the parameters listed in Table 2. They are 0.92 for Li^+ , 1.02 for Na^+ , 1.17 for Rb^+ , 1.43 for Cs^+ and 1.09 for ammonium. These numbers indicate that no large deviation from unity is expected when the constant energy peak offset condition is violated if the range of variation of the peak energies is narrow. In addition, there are problems in estimating G_m and K_m adjusting a hyperbola to the conductance-concentration relationship. Actually, the curve-relating conductance and concentration is not a hyperbola. The three-barrier model predicts a creep of the conductance as concentration increases, due to screening of the surface charges of the membrane (Cecchi et al., 1981). Because of these difficulties, this test cannot be taken as an additional demonstration of single-ion occupancy in the hemocyanin channel.

ENERGY WELLS

We now use the three-barrier model to account for the selectivity sequences found for the hemocyanin channel to alkali cations and ammonium ions. We want to use the parameters obtained from the three-barrier model not only as empirical values useful to characterize the relationships between conductance with voltage and concentration but also to gain some insight on the possible structure of the channel in terms of the characteristics of the binding sites.

The most prominent conclusion that is apparent from the inspection of the parameters presented in Table 2 is the sequence of energy values for the wells G_1 and G_2 . The parameters G_1 and G_2 are the free energies of transfer of an ion from the solution to that binding site in the channel. The order of free-energy change is $\text{Li}^+ > \text{Na}^+ > \text{K}^+ > \text{Rb}^+ > \text{Cs}^+$, which is expected for a strong

electric field binding site (Eisenmann, 1965). The interaction of the channel and the ion is strong enough to dehydrate the ion partially, and the selectivity sequence is that of the increasing dehydrated ionic radius, Li^+ being the more strongly bound ion and Cs^+ the least.

Ammonium ions can be used to probe the orientation of the ligands in the binding site, by comparing its binding energy to that of an alkali metal of the same size (Krasne & Eisenman, 1973). Thus, an enhanced NH_4^+ selectivity over cations of its same size (i.e., Rb^+) has been taken as an indication that there is favorable coordination between tetrahedrally oriented ligands and the tetrahedral distribution of charge on the NH_4^+ ion. We have found that ammonium binds to site 1 (cis well) more strongly than expected from its size, suggesting that the geometry of the ligands is tetrahedral. Despite the fact that both energy wells follow the same selectivity sequence for the alkali cations, we found that the trans well binds ammonium less tightly than the cis well, suggesting that this well has a different molecular arrangement.

ENERGY PEAKS

We have reported organic cation conductance measurements designed to probe the hemocyanin channel size (Cecchi et al., 1982) and our results indicate that ions the size of tetramethylammonium cannot cross the channel. Streaming potential experiments show that nonelectrolytes the size of urea are also excluded from the channel. These facts indicate that the narrowest part of the channel must be of the order of 0.25 nm in radius, a size consistent with the view that ions cross the hemocyanin channel in a partially dehydrated form. We have estimated the length of this narrow part of the channel to be 0.6 nm and we assume now, for the sake of the discussion, that most of the electric potential drops in this narrow part. If this assumption is granted, then the binding sites are located in this part of the channel, separated by 0.6 nm. If an ion is located midway between the two binding sites, it will be 0.3 nm away from the sites. This argument leads to a possible explanation of the physical meaning of the central energy barrier, following the proposition suggested by Hille (1975) which recognized that the same principles of Eisenman's *equilibrium* selectivity theory (e.g., Eisenman, 1965) could be applied to energy peaks. He pointed out that a barrier can be any dipolar or charged site that can attract the ion less than water does; i.e., "binding" to this site can be considered as the formation of a transition

state. (See Eisenman and Horn, 1983 for a detailed justification of Hille's hypothesis.) Therefore, we can expect the potential energy of the ion located midway to be that of the interaction with a large negative site (low field strength). This interpretation seems attractive since we have found for G_B , the energy barrier separating the wells, the selectivity sequence $\text{Na}^+ > \text{K}^+ > \text{Rb}^+ > \text{Cs}^+ > \text{Li}^+$ which is Eisenman's series VII arising from a site of lower field than the wells (Eisenman, 1965).

The outer energy barriers represent the motion of ions from the solutions to the binding sites. The access resistance to the channel does not appear to be playing a major role in this process because the sequence of the barrier height is not the one expected for free diffusion in water. For access from the cis side it is roughly the inverse, Li^+ being the ion that moves more freely and Cs^+ the more hindered. For the trans side, ammonium is the ion with the largest mobility and Li^+ that moving with more difficulty. Since the energy sequence for this step is $\text{Rb}^+ > \text{Cs}^+ \sim \text{K}^+ > \text{Na}^+ > \text{Li}^+$ (Eisenman's selectivity sequence II or III), it seems to involve a partial dehydration of ions and replacement of water by a low field strength group of the channel.

We acknowledge the able technical assistance of Mr. Juan Espinoza. We also acknowledge Drs. Dale Benos, Roberto Coronado, Christopher Miller and Cecilia Vergara for helpful criticism of the manuscript. The invaluable secretarial assistance of Marianita Sanchez is most appreciated. This work was supported by the Universidad de Chile, Departamento de Desarrollo de la Investigacion, Grant No. B-1224-822-3 and by NIH grants GM-25277 and GM-28992.

References

- Alvarez, O., Diaz, E., Latorre, R. 1975. Voltage-dependent conductance induced by hemocyanin in black lipid films. *Biochim. Biophys. Acta* **389**:444-448
- Alvarez, O., Latorre, R. 1978. Voltage-dependent capacitance in lipid bilayers made from monolayers. *Biophys. J.* **21**:1-17
- Alvarez, O., Reyes, J., Latorre, R. 1977. Ion transport through the hemocyanin channel. *Biophys. J.* **17**:754a (Abstr.)
- Antolini, R., Menestrina, G. 1979. Ion conductivity of the open keyhole limpet hemocyanin channel. *FEBS Lett.* **100**:377-381
- Cecchi, X., Alvarez, O., Latorre, R. 1981. A three-barrier model for the hemocyanin channel. *J. Gen. Physiol.* **78**:657-681
- Cecchi, X., Bull, R., Franzoy, R., Coronado, R., Alvarez, O. 1982. Probing the pore size of the hemocyanin channel. *Biochim. Biophys. Acta* **693**:173-176
- Coronado, R., Rosenberg, R.L., Miller, C. 1980. Ionic selectivity, saturation and block in a K^+ -selective channel from sarcoplasmic reticulum. *J. Gen. Physiol.* **76**:425-446
- Eisenman, G. 1965. Some elementary factors involved in specific ion permeation. *Excerpta Med. Int. Congr. Ser.* **87**:489-506
- Eisenman, G., Horn, R. 1983. Ionic selectivity revisited: The role of kinetic and equilibrium processes in ion permeation through channels. *J. Membrane Biol.* **76**:197-225

Hille, B. 1975. Ionic selectivity of Na^+ and K^+ channels of nerve membranes. In: *Membranes – A Series of Advances*, G. Eisenman, editor. Vol. 3, pp. 255–323. Marcel Dekker, New York

Krasne, S., Eisenman, G. 1973. The molecular basis of ion selectivity. In: *Membranes – A Series of Advances*, G. Eisenman, editor. Vol. 2, pp. 277–328. Marcel Dekker, New York

Lakshminarayanaiah, N. 1969. *Transport Phenomena in Membranes*. Academic, New York

Latorre, R., Alvarez, O., Ehrenstein, G., Espinoza, M., Reyes, J. 1975. The nature of the voltage-dependent conductance of the hemocyanin channel. *J. Membrane Biol.* **25**:163–182

Läuger, P. 1973. Ion transport through pores: A rate theory analysis. *Biochim. Biophys. Acta* **311**:423–441

Menestrina, G., Maniacco, D., Antolini, R. 1983. A kinetic study of the opening and closing properties of the hemocyanin channel in artificial lipid bilayer membranes. *J. Membrane Biol.* **71**:173–182

Pant, H.C., Conran, P. 1972. Keyhole limpet hemocyanin (KLH)-lipid bilayer membrane (BLM) interaction. *J. Membrane Biol.* **8**:357–362

Received 17 May 1983; revised 27 July 1983